Thermochimica Acta 502 (2010) 1–7

Contents lists available at ScienceDirect

Thermochimica Acta

journal homepage: www.elsevier.com/locate/tca

Morphology and thermal degradation behavior of highly exfoliated CoAl-layered double hydroxide/polycaprolactone nanocomposites prepared by simple solution intercalation

Hongdan Peng[a], Yu Han[a], Tianxi Liu[a,*], Wuiwui Chauhari Tjiu[b], Chaobin He[b]

[a] Key Laboratory of Molecular Engineering of Polymers of Ministry of Education, Department of Macromolecular Science, Laboratory of Advanced Materials, Fudan University, 220 Handan Road, Shanghai 200433, PR China
[b] Institute of Materials Research and Engineering, A*STAR (Agency for Science, Technology and Research), 3 Research Link, Singapore 117602, Singapore

ARTICLE INFO

Article history:
Received 29 November 2009
Received in revised form
26 December 2009
Accepted 2 January 2010
Available online 13 January 2010

Keywords:
Polycaprolactone
Layered double hydroxide
Nanocomposites
Thermal degradation

ABSTRACT

Highly exfoliated CoAl-layered double hydroxide (CoAl-LDH)/polycaprolactone (PCL) nanocomposites were successfully synthesized by simple solution intercalation of PCL into the galleries of organically modified CoAl-LDH (OCoAl-LDH) under reflux in cyclohexanone. The structure and thermal properties of the nanocomposites were characterized by Fourier Transform Infrared spectroscopy (FTIR), X-ray diffraction (XRD), Transmission Electron Microscopy (TEM), Thermal Gravimetry Analysis (TGA) and Differential Scanning Calorimetry (DSC). TGA data show that the thermal degradation temperature of the PCL nanocomposite with the addition of 1 wt% of LDH is lowered by 18 °C as compared to that of neat PCL. Dynamic FTIR spectra, coupled with two-dimensional infrared (2D-IR) correlation spectra, clearly reveal that the decrease in the degradation temperature observed for the nanocomposites is not just due to the decomposition of OCoAl-LDH at low temperature, but also mainly due to the negative catalytic degradation effect of OCoAl-LDH, where the ester groups of PCL matrix are catalytically hydrolyzed by the hydroxyl groups on LDH surface.

1. Introduction

Nanocomposites are two phase materials in which the inorganic filler particles have at least one dimension with nanometer from 0.1 to 100 nm range [1]. Layered double hydroxides (LDHs), being layered crystalline materials with easily exchangeable interlayer ionic species, can act as host matrices for the intercalation of organic polymers in order to synthesize hybrid organic–inorganic nanocomposites [2]. In recent years, polymer/LDH nanocomposites have attracted considerable interest in the field of material chemistry [3–6]. Owing to their novel mechanical, optical and thermal properties which are rarely present in neat polymers or micro-scale composites, these hybrids may have wide range of applications such as organoceramics, biomaterials, electrical and mechanical materials [2,7–12]. In general, the performance of these unique properties depends mainly on the dispersion degree (intercalation or exfoliation) of LDH layers in the polymer matrices [13]. From these two types of nanocomposites, the exfoliated one usually attracts more interest since better dispersion of LDH layers in polymer matrix results in enhanced properties as compared to the intercalated nanocomposites [14]. However, LDH layers have high charge density (ca. 300 mequiv./100 g) and strong interlayer electrostatic interaction which makes the exfoliation of LDH to be much more difficult [15]. In addition, pristine LDH is not suitable for the penetration of giant polymer chains or chain segments into their gallery space unless its interlayer distance is significantly increased. Accordingly, the intercalation of LDH involves organic modification of LDH to expand the basal spacing and/or ionogenic modification of the polymer to graft anions onto the polymers or monomers [16]. Previous studies have shown that polymer/LDH nanocomposites are generally prepared via three main pathways as follows: direct intercalation, in situ polymerization and restacking process [17].

Polycaprolactone (PCL), being one of the most important biocompatible and biodegradable aliphatic polyester, provides many potential biomedical and packaging applications, such as the matrix material for bone substitutes, scaffolds, drug carriers for controlled release, and food packaging [18–20]. However, the applications for such polymers are limited due to their poor mechanical and water vapour (as well as other gases) barrier properties. PCL/clay nanocomposites have usually demonstrated improved properties as compared with neat PCL [21–24]. In contrast to layered clay, LDH particles are constituted of metal hydroxide layers which display a positively surface charge where it is counter-balanced by anions located in the domains between adjacent layers. LDH materials can

* Corresponding author. Tel.: +86 21 5566 4197; fax: +86 21 6564 0293.
E-mail address: txliu@fudan.edu.cn (T. Liu).

0040-6031/$ – see front matter © 2010 Elsevier B.V. All rights reserved.
doi:10.1016/j.tca.2010.01.009

accommodate a wide range of different anions and cations, leading to a large compositional variety and thus tunability for a large number of applications [25–27]. One main area that has been the focus of intense research in recent years is the use of LDH as host matrices for the storage and delivery devices for biological implant. Furthermore, the wide range of varieties of cations that can consist of an LDH means that it is facile to produce biocompatible materials [28]. This is similar to the hydroxylapatite-reinforced biodegradable polyester nanocomposites [29]. The biodegradable polymers filled with LDH will be a potential biocompatible nanocomposites, which can possibly widen the applications of biodegradable polymers as the biomedical materials [30].

Till now, there are few reports on PCL/LDH composites [1,31–35]. Vittoria et al. have reported the preparation of PCL composites reinforced with 12-hydroxydodecanoate (HD) anions modified MgAl-LDH (MgAl-LDH-HD) by using high energy ball milling (HEBM) technique [32]. HEBM is an effective and unconventional technique currently used in inorganic material systems and processing. It was observed that the mechanical and other physical properties (such as the modulus and stress at yield as well as the barrier property) of the composites were enhanced in comparison with the neat PCL. Very recently, the same research group succeeded in incorporating nitrate form of MgAl-LDH by ionic exchange procedure into a chemically modified PCL. X-ray diffraction and AFM analysis suggested possible formation of partially exfoliated nanocomposites [1]. Unfortunately, all the preparation approaches reported previously, such as direct melt blending of PCL with MgAl-LDH-HD, in situ polymerization of ε-caprolactone in the presence of MgAl-LDH-HD, or mixing THF solution of PCL with MgAl-LDH-HD, are unable to successfully achieve PCL/LDH nanocomposites because the MgAl-LDH-HD microcrystals remain to be an essential integral within the polymeric matrix [31]. Therefore, a convenient and efficient method to synthesize exfoliated PCL/LDH nanocomposites is undoubtedly a rewarding and challenging work.

As compared to MgAl-LDH, transition-metal-bearing LDHs (such as Co–Al and Fe–Al) are known to have wider technological applications due to their unique catalytic, electronic, optical, and magnetic properties [36–39]. Therefore, it may be desirable to obtain their new, interesting hybrid polymeric materials. In this paper, the highly exfoliated CoAl-LDH/PCL nanocomposites were obtained for the first time by simply refluxing the mixture of dodecyl sulfate modified CoAl-LDH (OCoAl-LDH) and PCL in cyclohexanone solution. The nanostructure and thermal degradation mechanism of the exfoliated CoAl-LDH/PCL nanocomposites were also investigated.

2. Experimental

2.1. Materials

PCL (number-average molecular weight = 80,000 Da, Aldrich), $CoCl_2 \cdot 6H_2O$, $AlCl_3 \cdot 6H_2O$ and urea (analytical purity) were supplied by Shanghai Zhenxing Chemicals. Sodium dodecyl sulfate (SDS), NaCl and cyclohexanone (analytical purity) were obtained from China Medicine (Group) Shanghai Chemical Reagent Corporation. All these commercial chemicals were used as received without further purification.

2.2. Preparation of samples

Dodecyl sulfate modified CoAl-LDH (OCoAl-LDH) was obtained according to the procedure reported previously [39]. The PCL/CoAl-LDH nanocomposites were prepared by the solution intercalation method. Firstly, a desired amount of OCoAl-LDH was sonicated at a frequency of 40 kHz for 0.5 h and refluxed in 50 mL cyclohexanone for 12 h under flowing nitrogen. Subsequently, this solution was added to the PCL solution in 50 mL cyclohexanone and refluxed for another 12 h. Finally, the solution was poured into 300 mL cool methanol. The precipitates, PCL/CoAl-LDH nanocomposites, were filtered and dried under vacuum at 40 °C for 48 h. The dried nanocomposites were made into thin sheets with thickness of 0.5 mm by compression molding at 100 °C using a Carver laboratory press, followed by rapid quenching in an ice/water bath. Similar preparation conditions were used for each composition of the materials containing 0, 1, 2, 4 wt% of OCoAl-LDH.

2.3. Characterization

FTIR spectra were recorded on a Nexus 470 FTIR spectrophotometer (Nicolet Instruments, USA). FTIR samples were prepared in the form of KBr disks or thin films. XRD patterns of the samples were obtained by X'Pro X-ray diffractometer with Cu Kα radiation (λ = 0.1548 nm) under a voltage of 40 kV and a current of 40 mA. The samples were scanned over the range of 2θ from 2.5° to 50°, with a scan speed of 0.5°/min at room temperature. Ultrathin sections for TEM observations were prepared by sectioning the sample with diamond knife at room temperature to thickness of 50–70 nm using a Leica ultramicrotome. The ultrathin films were mounted on carbon coated copper grids and observed using TEM (JEOL JEM-2100 TEM) under an accelerating voltage of 200 kV.

TGA was performed under nitrogen flow from 50 to 600 °C at a heating rate of 10 °C/min using a Perkin Elmer TGA 7. DSC experiments were performed under nitrogen environment by a TA DSC 2920. The melting and crystallization studies were performed in the temperature range of 0–100 °C at a heating rate of 10 °C/min, and hold isothermally at 100 °C for 3 min to eliminate the thermal history. The samples were then cooled to 0 °C at a cooling rate of 10 °C/min. The DSC curves were recorded and analyzed.

The real-time FTIR spectra were recorded with a 4 cm^{-1} spectra resolution on a Nicolet Nexus 470 spectrometer equipped with a DTGS detector by signal averaging 64 scans. The baseline correction was done by using OMNIC 6.1 software. The film samples were placed in a ventilated oven at a heating rate of 10 °C/min for the dynamic measurements of FTIR spectra during the thermo-oxidative degradation. The relative concentrations of alkyl and carbonyl groups were calculated from the intensity ratios of peak heights at 150 °C to the maximum heights of the 2943 and 1735 cm^{-1} peaks. Repeated experiments showed that small variations in sample thickness had no significant influence on the relative peak intensity.

The real-time FTIR spectra were recorded at a temperature interval of 10 °C and the generalized two-dimensional (2D) correlation analyses in selected range of wavenumber were analyzed by using 2D Shige software developed by Shigeaki Morita (Kwansei-Gakuin University, Japan). In 2D correlation maps, the red-colored regions are defined as the positive correlation intensities, whereas the blue-colored ones are regarded as the negative correlation intensities.

3. Results and discussion

3.1. FTIR characterization of PCL/CoAl-LDH nanocomposites

Fig. 1 compares the FTIR spectra of OCoAl-LDH, neat PCL, and PCL nanocomposite containing 4 wt% LDH samples. The assignment of the bands was based on previous assignments as reported in the literature [40]. The OCoAl-LDH sample (Fig. 1a) has a broad adsorption band around 3500 cm^{-1} due to O–H stretching modes of interlayer water molecules and H-bonded OH groups. The corresponding bending mode of water molecules appears at about 1630 cm^{-1}.

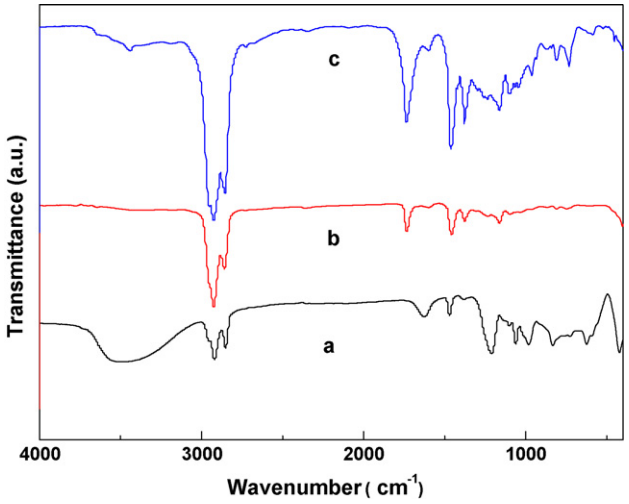

Fig. 1. FTIR spectra of (a) OCoAl-LDH, (b) neat PCL and (c) PCL/OCoAl-LDH (4 wt%) nanocomposites.

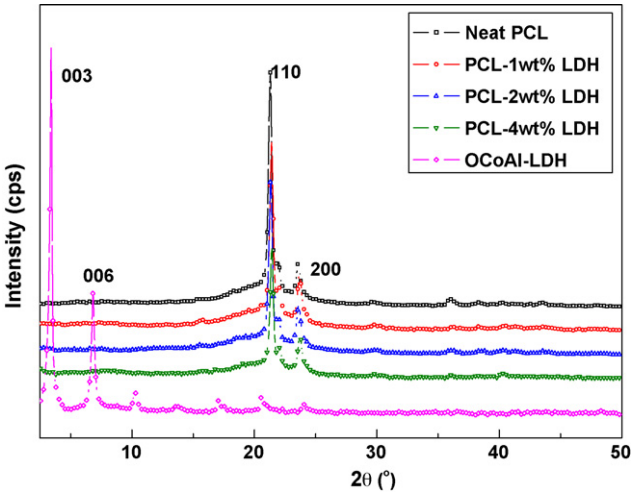

Fig. 2. XRD patterns of OCoAl-LDH, neat PCL and PCL/CoAl-LDH nanocomposites with different LDH loadings.

The C–H stretching vibration at 2848, 2920, and 2957 cm^{-1} and the stretching vibration of sulfate from dodecyl sulfate anion at 1218 cm^{-1} can also be observed. In addition, the absorbance bands in the range of 800–400 cm^{-1} region are due to the lattice vibration bands of the M–O and O–M–O (where M = Co, Al) groups. These features are in good agreement as reported in literature [39]. The principal bands of pure PCL are 3000–2800 cm^{-1} (CH_2 stretching vibrations), 1735 cm^{-1} (C=O stretching vibrations), 1275–1050 cm^{-1} (C–O–C aliphatic ether stretching vibrations), 730 cm^{-1} (CH_2 long chain rocking motion vibrations), and 1450 and 1380 cm^{-1} (CH_2 and CH bending vibrations). Taking neat PCL sample (Fig. 1b) as comparison, the PCL nanocomposite with 4 wt% CoAl-LDH (Fig. 1c) shows some new absorption peaks at 3100–3600 cm^{-1} (O–H stretching vibrations), and 1640 cm^{-1} (H–O–H bending vibrations), respectively. The lattice vibration bands below 800 cm^{-1}, which is absent in the pristine PCL sample, also unequivocally provide an evidence that the LDH layers have been doped into the PCL matrix by the solution intercalation thus forming the PCL/CoAl-LDH nanocomposites.

3.2. Structure and morphology of exfoliated PCL/CoAl-LDH nanocomposites

Fig. 2 shows the XRD patterns for 2θ range from 2.5° to 50° for OCoAl-LDH, neat PCL and their corresponding PCL/OCoAl-LDH nanocomposites. Pristine PCL shows reflection peaks at $2\theta = 21.3°$ and 23.7°, which correspond to (1 1 0) and (2 0 0) crystallographic planes of PCL, respectively. The (0 0 3) basal spacing (d_{003}) of OCoAl-LDH powder sample, calculated from the diffraction peak at $2\theta = 3.46°$, is 2.53 nm, which is consistent with the value reported elsewhere [39]. This indicates that a swollen and intercalated structure is successfully formed by the insertion of the surfactant (SDS) into the host gallery of the LDH platelets without destructing the regular, alternating stacking of the LDH layers. However, this peak is not present in the nanocomposite samples. Therefore, the complete disappearance of the basal plane of LDH may be due to the collapse of the stacked lamellar LDH structure, leading to the formation of disordered and exfoliated nanostructure within the matrix. In other words, the LDH platelets are randomly dispersed throughout the PCL matrix. The two sharp reflection peaks of PCL at $2\theta = 21.3°$ and 23.7° can still be observed in all the nanocomposites.

Although XRD could provide a partial picture about the distribution of nanofillers, a complete morphology characterization of nanocomposites usually requires microscopic investigation. TEM analysis allows a direct visualization of the morphology, spatial distribution and dispersion of the nanoparticles or platelets within the polymer matrices. Fig. 3a shows low magnification TEM image of PCL nanocomposite containing 4 wt% OCoAl-LDH. The dark lines represent the LDH layers, whereas the gray areas correspond to the polymer matrix. The image clearly reveals that OCoAl-LDH layers have completely lost their stacking orders and are inhomogeneously distributed in the continuous polymer matrix. The absence of aggregates confirms the high degree of exfoliation of

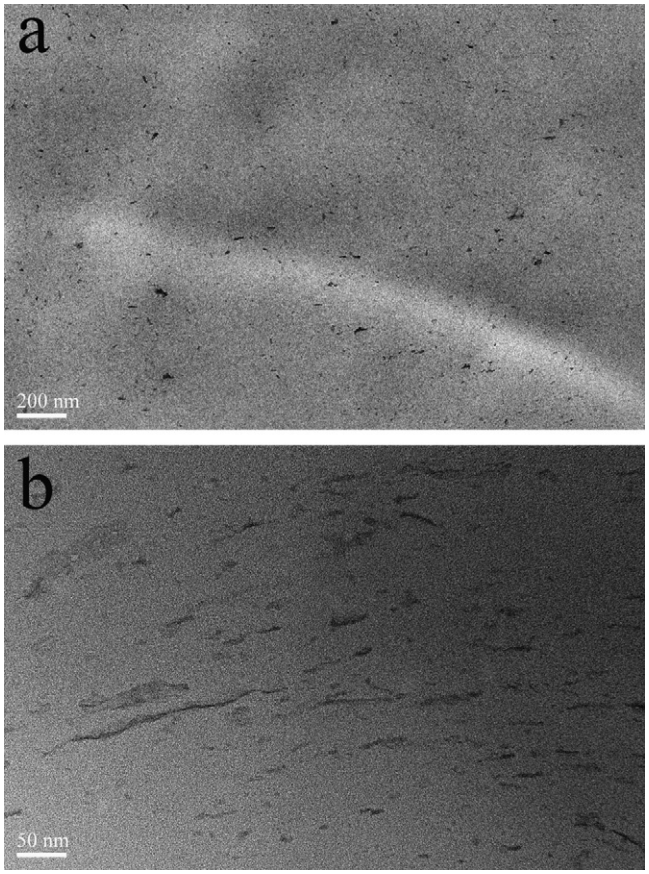

Fig. 3. TEM images of PCL nanocomposite with 4 wt% CoAl-LDH: (a) at low magnification and (b) at high magnification.

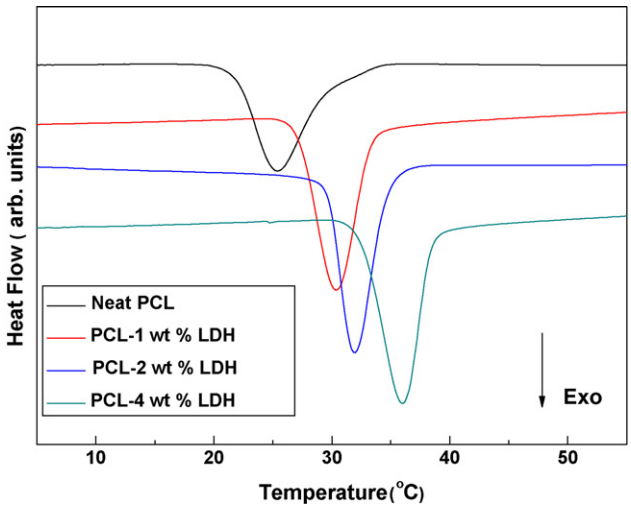

Fig. 4. DSC cooling scans at cooling rate of 10 °C/min for neat PCL and PCL/CoAl-LDH nanocomposites with different contents of OCoAl-LDH.

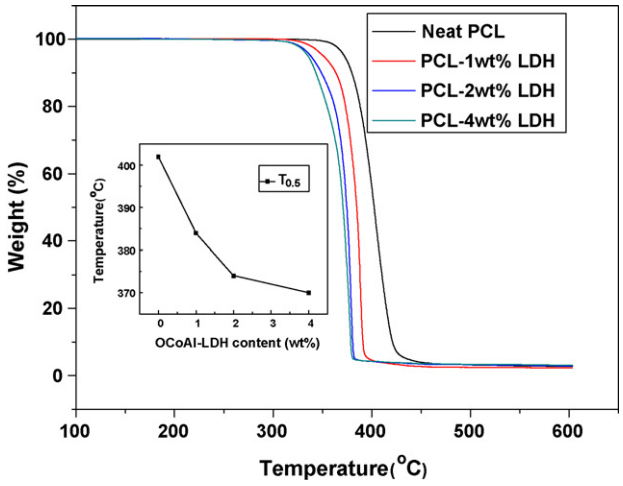

Fig. 5. TGA profiles for neat PCL and PCL/CoAl-LDH nanocomposites with different loadings of OCoAl-LDH in nitrogen atmosphere with a heating rate of 10 °C/min. The inset shows the thermal decomposition temperature at 50% weight loss ($T_{0.5}$) of neat PCL and its nanocomposites with different loadings of OCoAl-LDH.

the LDH platelets within PCL. TEM image at higher magnification (Fig. 3b) shows the diffuse nature of the nanoplatelets which vary widely in size and shape. It is worth noting that a large number of LDH platelets with dimension of 10–20 nm appear in the sample, this may be due to the breakage of CoAl layers when being refluxed in cyclohexanone. Chen and Qu have reported similar results from polyethylene/ZnAl-LDH nanocomposites synthesized in xylene under reflux treatment [16]. In fact, the exfoliated NO_3^-CoAl-LDH layers in formamide (even at room temperature) are also morphologically irregular and dimensionally diminished in comparison with the parent LDH crystallites [39]. The layer-breaking process during the delamination may destroy the crystal structure of LDH and facilitate the penetration of polymer chains into the center of OCoAl-LDH sheets, thus lead to the formation of exfoliated structures. The exfoliated morphology observed here by TEM is in good agreement with the XRD results.

3.3. Thermal properties of PCL/CoAl-LDH nanocomposites

To elucidate the effect of LDH on crystallization behavior of PCL matrix, thermal analysis was performed by DSC. Fig. 4 shows the DSC cooling curves of neat PCL and its nanocomposites. It can be seen that, the exothermic peak for neat PCL is located at 25 °C. As the OCoAl-LDH loading increases, the melt crystallization temperature increases gradually, and the addition of 4 wt% OCoAl-LDH results in an increase of the crystallization temperature of PCL nanocomposite by 36 °C. The increase in crystallization temperature with the incorporation of LDH into PCL matrix is due to the fact that LDH can act as nucleating agent which has a heterogeneous nucleation effect.

Fig. 5 illustrates the TGA curves in nitrogen atmosphere for neat PCL and its nanocomposites with different loadings of OCoAl-LDH. It is obvious to note that the degradation of nanocomposites occurs at lower temperature as compared to the neat PCL and the thermal degradation temperature decreases gradually with the increase of OCoAl-LDH loading level. When 50% weight loss was selected as the point of comparison, the thermal decomposition temperatures ($T_{0.5}$) for neat PCL and its nanocomposites containing 1, 2 and 4 wt% LDH were determined to be 402, 384, 374, 370 °C, respectively. Vittoria et al. also reported similar results for MgAl-LDH and its chemically modified PCL systems [1]. According to them, this reverse trend in thermal stability is due to the presence of MgAl-LDH-HD in the PCL composite samples, which had been shown to degrade at lower temperatures than neat PCL. However, in most cases, it is known that the thermal stability of the polymer/LDH nanocomposites will increase as compared with its corresponding LDH-free polymer matrices [25]. For example, it was reported that the addition of the LDH to PMMA resulted in an increase in thermal stability of the composites and does not affect the degradation steps of PMMA [26,27]. It has been reported that the beneficial effect of LDH on the thermal stability of polymer matrix is due to the promotion of the charring process of the matrix and the barrier effect of LDH layers for the diffusion of oxygen and volatile products throughout the composite materials during the thermal decomposition of the composites [41].

As mentioned above, to eliminate the stronger electrostatic interactions between the LDH layers and to obtain the intercalated or exfoliated nanostructure, the surfactants are usually used to modify the surface property of the LDH layers, which has been proven to be an effective method [42,43]. Similarly in this study, we first obtained surfactant-modified CoAl-LDH (OCoAl-LDH). Therefore, the decomposition of OCoAl-LDH plays an important role in the thermal decomposition of exfoliated CoAl-LDH/PCL nanocomposites. Fig. 6 gives the TGA and the corresponding derivative thermogravimetric (DTG) curves of OCoAl-LDH under nitrogen atmosphere. The weight loss at temperatures below 200 °C can be assigned to the removal of interlayer water molecules and the thermal decomposition of LDH layers via the removal of –OH groups

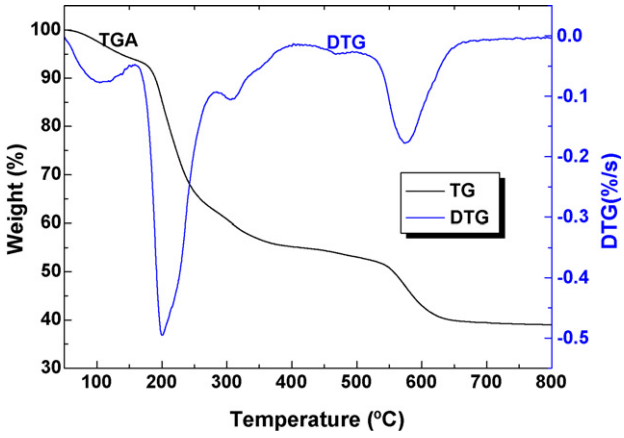

Fig. 6. TGA and DTG curves of the OCoAl-LDH sample in nitrogen atmosphere with a heating rate of 10 °C/min.

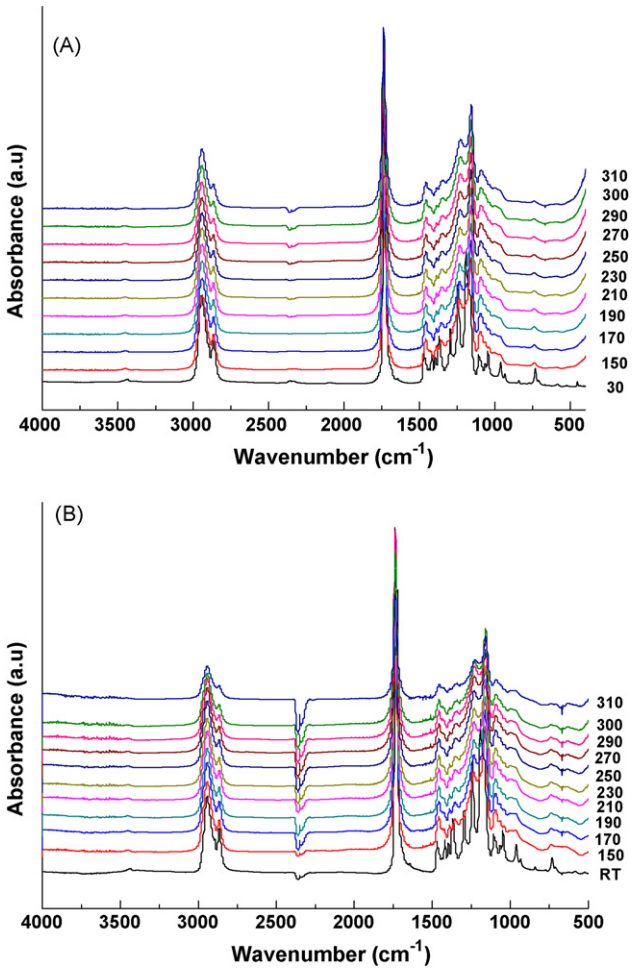

Fig. 7. Dynamic FTIR spectra at different thermo-oxidative temperatures: (a) neat PCL; (b) PCL nanocomposite with 4 wt% LDH.

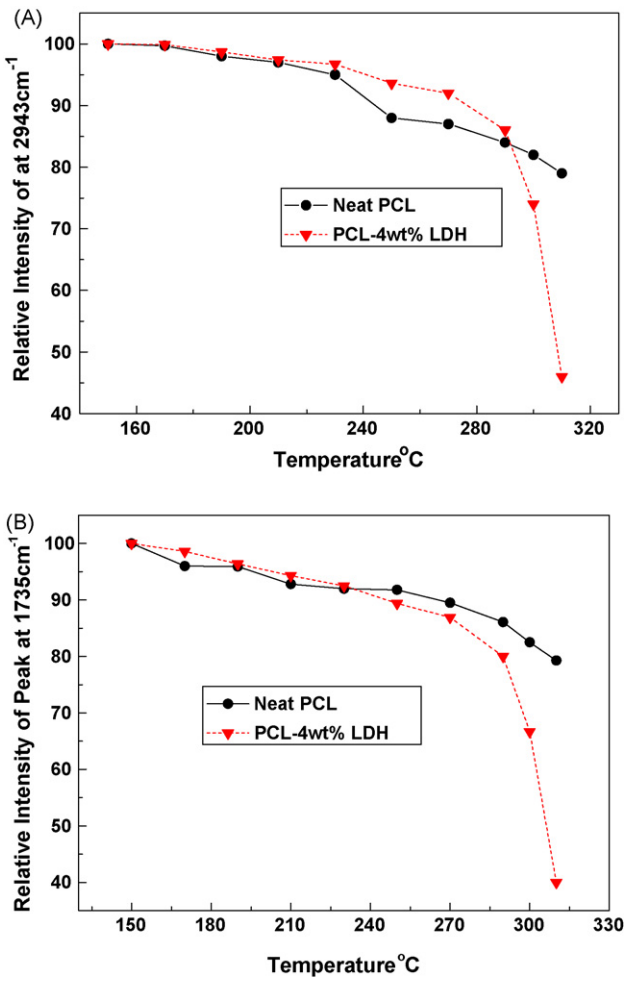

Fig. 8. Changes of the relative peak intensities at 2943 cm^{-1} (a) and 1735 cm^{-1} (b) with different thermo-oxidative temperatures.

in the form of water molecules. The later stages of weight loss at around 305 °C are probably due to the degradation of the interlayer dodecyl sulfate (DS) anions. After the thermal decomposition of the organics up to 800 °C, LDH materials are transformed into Co–Al oxides. Ding et al. [3] clearly demonstrated the effects of the small organic molecules and the dispersion of the LDH layers on the thermal properties of polystyrene (PS) nanocomposites. Their results showed that SDS-modified LDH, which was shown to degrade at lower temperature due to the decomposition of the short alkyl chains of SDS, can significantly enhance the thermal stability of PS matrix when 50% weight loss was selected as a point of comparison. According to Chen et al. [44], when the MgAl-DS component begins to degrade due to the loss of hydroxide on MgAl hydroxide layers from ca. 150 °C, the hydroxide on MgAl hydroxide layers in PMMA nanocomposites does not degrade until the temperature reaches 200 °C due to the protection by intercalated PMMA chains in the gallery of MgAl hydroxide layers. Similarly, the degradation behavior of PCL and its nanocomposites at lower temperatures is almost identical. This is probably due to the polar interactions between PCL chains and OCoAl-LDH nanoparticles, which play an important role on the intercalation of polymer chains within the LDH layers, protect the dehydrated CoAl hydroxide layers.

Till now, the mechanisms of the thermal stability and degradation of polymer nanocomposites are still not clearly understood. Many studies have suggested that the effect may be associated with the chemical interaction between the polymer matrix and the surface of clay layers during the thermal degradation and combustion processes. Zanetti et al. reported the catalytic effect of the nanodispersed clay layers in PP/MMT (montmorillonite) and EVA/MMT nanocomposites [45,46]. It has also been found that the structural iron in clays could act as a radical trap to prevent degradation [47]. It is well known that the LDHs have a very wide range of chemical compositions based on different type of metal species, interlayer anions, etc. and are frequently used as catalysts, catalyst supports in numerous reactions [48]. For example, the surface alkalinity of the LDHs results in high catalytic activities for the epoxidation of olefins [49], N-oxidation of pyridines [50], and C–C bond-forming reactions [51]. And, the Fe^{3+} cations could prevent nanocomposites from decomposing by radical trapping at the onset temperature region in MgFe/PMMA nanocomposites [52]. That is to say, the chemical interaction between the polymer matrix and the LDH layer surface played a very important role during thermal degradation and combustion processes. Therefore, it is reasonable to deduce that the unusual thermal degradation behavior of PCL/OCoAl-LDH nanocomposites may also be due to the chemical interaction between the OCoAl-LDH and PCL matrix, i.e. the negative effect of catalytic degradation as a weak alkaline for the OCoAl-LDH. In order to better understand the mechanism for the decrease in thermal stability of the PCL/LDH nanocomposites as observed in this study, dynamic FTIR and 2D-IR analysis have been used to investigate the structural changes during the thermo-oxidative degradation processes.

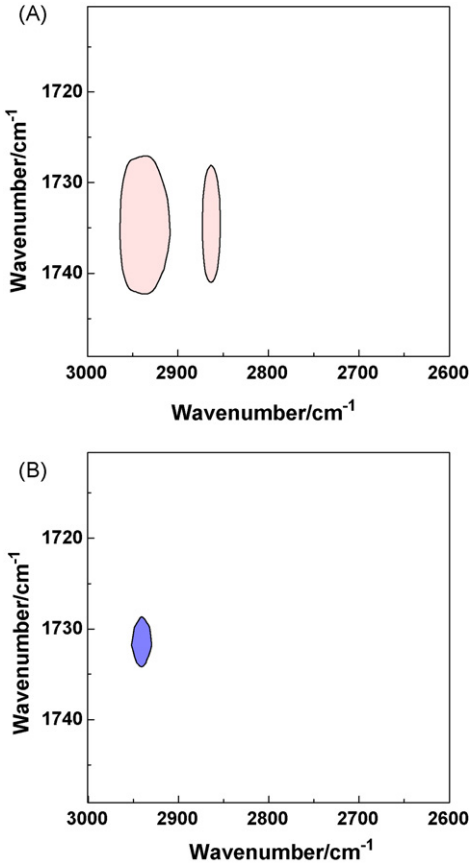

Fig. 9. Synchronous (a) and asynchronous (b) 2D correlation spectra (3000–1715 cm^{-1}) calculated from the temperature dependent FTIR spectra of PCL nanocomposite with 4 wt% LDH in nitrogen in the temperature range of 150–310 °C.

3.4. Thermal oxidation behavior of PCL/CoAl-LDH nanocomposites

Dynamic FTIR can provide detailed information on structural evolution at the molecular level during the thermo-oxidative degradation process [53]. Fig. 7 shows the changes of dynamic FTIR spectra obtained from the thermo-oxidative degradation of neat PCL (Fig. 7a) and its nanocomposite with 4 wt% CoAl-LDH loading (Fig. 7b) from room temperature (R.T.) to 310 °C. The peaks at 2943 and 2854 cm^{-1} are assigned to CH_2 or CH_3 asymmetric and symmetric stretching vibrations, respectively. The intensities of these two peaks decrease as the thermo-oxidative degradation temperature increases due to the decomposition of PCL main chains. A two-stage degradation mechanism for neat PCL has been proposed by Persenaire et al. [54]. The first stage implies a statistical rupture of the polyester chains via ester pyrolysis reaction. The second stage leads to the formation of ε-caprolactone (cyclic monomer) as a result of an unzipping depolymerization process. The band at 1735 cm^{-1}, which correspond to C=O stretching vibration, is also an interesting region. Although the dynamic FTIR spectra in Fig. 7a and b show very similar features, apart from some absorption peaks of nanofiller, the rate of change of their peak intensities as the pyrolysis temperature increases is completely different.

Fig. 8 shows the changes of the relative peak intensities at 2943 and 1735 cm^{-1} with the pyrolysis temperature for neat PCL and its CoAl-LDH nanocomposites. From R.T. to about 220 °C, the thermo-oxidation is almost the same as that of neat PCL. Above 250 °C, the relative peak intensities of the nanocomposites at 2943 and 1735 cm^{-1} are much lower than those of PCL, implying a catalytic degradation effect due to the presence of OCoAl-LDH.

Generalized 2D correlation spectroscopy, which was first proposed by Noda, is a versatile tool for the analysis of a set of spectroscopic data obtained from a system under certain type of external perturbation [55–57]. Two types of spectra, 2D synchronous and asynchronous spectra, are obtained in general. With the cross-peaks both in synchronous and asynchronous maps, one can get the specific order of the spectral intensity changes that take place while the sample is subjected to an environmental perturbation [58,59]. Fig. 9 presents the synchronous (a) and asynchronous (b) 2D correlation spectra (3000–1700 cm^{-1}) for the thermal degradation process of PCL nanocomposite containing 4 wt% LDH in nitrogen atmosphere in the temperature range of 150–310 °C. As explained by the rule proposed by Noda [56], the symbols of the cross-peak at (2943, 1735 cm^{-1}) are respectively positive and negative in the synchronous and asynchronous maps, inferring that when heated, carbonyl decomposes faster than alkyl groups. This means that in PCL/CoAl-LDH nanocomposites, polyester chains will be the first to decompose, followed by the gradual chain scission of C–H and C–C main chains of PCL.

All these results show that although the disorderedly dispersed OCoAl-LDH layers in the PCL matrix at the nanoscopic scale can hinder the escape of degenerated small molecules which leads to the improvement in the thermal properties, but at the same time the LDH layer can directly catalyze the carbonyl decomposition during the thermal degradation which results in the decrease in degradation temperature with the increase of OCoAl-LDH loading level.

4. Conclusions

A facile procedure was developed to prepare exfoliated PCL/CoAl-LDH nanocomposites by solution intercalation of PCL chains into organically modified CoAl-LDH interlayers in cyclohexanone. The nanoscale dispersion of CoAl-LDH layers in the PCL matrix has been verified by the disappearance of the d_{003} XRD diffraction peak and TEM micrographs. DSC data give evidence that the exfoliated LDH layers have heterogeneous nucleation effect on the crystallization of PCL and its crystallization temperature is increased by more than 10 °C with the addition of merely 4 wt% OCoAl-LDH. The TGA profiles of the PCL/CoAl-LDH nanocomposites show that a small amount of OCoAl-LDH can significantly decrease the thermal stability of exfoliated PCL nanocomposites. This is because LDH has negative catalytic degradation effect on the PCL resin in addition to its barrier effect for enhanced thermal stability. These two competing effects in the PCL nanocomposites are well demonstrated by dynamic FTIR and 2D correlation spectroscopy analysis. From our results, we conclude that the surface alkalinities of the CoAl-LDH, which can hydrolytically cleave the ester groups of PCL, are the main reason for the decrease in thermal stability of PCL nanocomposites. This type of exfoliated nanocomposites is promising for the application of magnetic, biological, medical, and flame-retardant polymeric materials. Currently, we are still investigating whether the delamination process of CoAl-LDH is also applicable to other LDH materials and further exploring their properties and applications.

Acknowledgements

This work is supported by the National Natural Science Foundation of China (20774019; 50873027), “Shu Guang” project supported by Shanghai Municipal Education Commission and Shanghai Education Development Foundation, and the Shanghai Leading Academic Discipline Project (Project Number: B113).

References

[1] P. Mangiacapra, M. Raimondo, L. Tammaro, V. Vittoria, Biomacromolecules 8 (2007) 773–779.
[2] E.R. Hitzky, M. Darder, P. Aranda, J. Mater. Chem. 15 (2005) 3650–3662.
[3] P. Ding, M. Zhang, J. Gai, B.J. Qu, J. Mater. Chem. 17 (2007) 1117–1122.
[4] S. O'Leary, D. O'Hare, G. Seeley, Chem. Commun. 14 (2002) 1506–1507.
[5] F. Leroux, C.T. Gueho, J. Mater. Chem. 15 (2005) 3628–3642.
[6] M.C. Nshuti, D.Y. Wang, J.M. Hossenlopp, C.A. Wilkie, J. Mater. Chem. 18 (2008) 3091–3102.
[7] P.B. Messersmith, S.I. Stupp, Chem. Mater. 7 (1995) 454–460.
[8] M. Darder, P. Aranda, E.R. Hitzky, Adv. Mater. 19 (2007) 1309–1319.
[9] M.M.E. Jacob, E. Hackett, E.P. Giannelis, J. Mater. Chem. 13 (2003) 1–5.
[10] H.B. Hsueh, C.Y. Chen, Polymer 44 (2003) 5275–5283.
[11] W.D. Lee, S.S. Im, H.M. Lim, K.J. Kim, Polymer 47 (2006) 1364–1371.
[12] F. Leroux, J. Gachon, J.P. Besse, J. Solid State Chem. 177 (2004) 245–250.
[13] P. Ding, B.J. Qu, J. Polym. Sci. B: Polym. Phys. 44 (2006) 3165–3172.
[14] T. Kuila, H. Acharya, S.K. Srivastava, A.K. Bholomica, J. Appl. Polym. Sci. 108 (2008) 1329–1335.
[15] M. Darder, M. Blanco, P. Aranda, F. Leroux, E.R. Hitzky, Chem. Mater. 17 (2005) 1969–1977.
[16] W. Chen, B.J. Qu, J. Mater. Chem. 14 (2004) 1705–1710.
[17] F. Leroux, J.P. Besse, Chem. Mater. 13 (2001) 3507–3515.
[18] G. Gorrasi, V. Vittoria, E. Pollet, M. Alexandre, P. Dubois, J. Polym. Sci. B: Polym. Phys. 42 (2004) 1466–1475.
[19] J. John, J. Tang, Z. Yang, M. Bhattacharya, J. Polym. Sci. A: Polym. Chem. 35 (1997) 1139–1148.
[20] L. Liao, C. Zhang, Q. Gong, Macromol. Rapid Commun. 28 (2007) 1148–1154.
[21] B. Lepoittevin, N. Pantoustier, M. Alexander, C. Calberg, R. Jerome, P. Dubois, J. Mater. Chem. 12 (2002) 3528–3532.
[22] P. Viville, R. Lazzaroni, E. Pollet, M. Alexandre, P. Dubois, J. Am. Chem. Soc. 126 (2004) 9007–9012.
[23] V.M. Karauan, E.G. Privalko, V.P. Privalko, D. Kubies, R. Puffr, R. Jerome, Polymer 46 (2005) 1943–1948.
[24] B. Chen, R.G. Evans, Macromolecules 39 (2006) 747–754.
[25] S. Tsukamoto, A. Kuma, M. Murakami, C. Kishi, A. Yamamoto, N. Mizushima, Science 321 (2008) 113–117.
[26] C.M. Nshuti, P. Songtipya, E. Manias, M.M. J-Gasco, J.M. Hossenlopp, C.A. Wilkie, Polymer 50 (2009) 3564–3574.
[27] C. Nyambo, D. Chen, S. Su, C.A. Wilkie, Polym. Degrad. Stab. 94 (2009) 1298–1306.
[28] G.R. Williams, D. O'Hare, J. Mater. Chem. 16 (2006) 3065–3074.
[29] N. Ignjatovic, S. Tomic, M. Dakic, M. Miljkovic, M. Plavsic, D. Uskokovic, Biomaterials 20 (1999) 809–816.
[30] P. Pan, B. Zhu, T. Dong, Y. Inoue, J. Polym. Sci. B: Polym. Phys. 46 (2008) 2222–2233.
[31] L. Tammaro, M. Tortora, V. Vittoria, U. Costantino, F. Marmottini, J. Polym. Sci. A: Polym. Chem. 43 (2005) 2281–2290.
[32] A. Sorentino, G. Gorrasi, M. Tortora, V. Vittoria, U. Costantino, F. Marmottinic, F. Padella, Polymer 46 (2005) 1601–1608.
[33] R. Pucclariello, L. Tammaro, V. Villani, V. Vittoria, J. Polym. Sci. B: Polym. Phys. 45 (2007) 945–954.
[34] V. Romeo, G. Gorrasi, V. Vittoria, Biomacromolecules 8 (2007) 3147–3152.
[35] U. Costantino, V. Bugatti, G. Gorrasi, F. Montanari, M. Nocchetti, L. Tammaro, V. Vittoria, ACS Appl. Mater. Interfaces 1 (2009) 668–677.
[36] R. Xu, H.C. Zeng, Chem. Mater. 13 (2001) 297–303.
[37] G.A. Caravaggio, C. Detellier, Z. Wronski, J. Mater. Chem. 11 (2001) 912–921.
[38] X.M. Liu, Y.H. Zhang, X.G. Zhang, S.Y. Fu, Electrochim. Acta 49 (2004) 3137–3141.
[39] Z.P. Liu, R.Z. Ma, M. Osanda, N. Iyi, Y. Ebina, K. Takada, T. Sasaki, J. Am. Chem. Soc. 128 (2006) 4872–4880.
[40] P. Viville, R. Lazzaroni, Langmuir 19 (2003) 9425–9433.
[41] L.Z. Qiu, W. Chen, B.J. Qu, Polymer 47 (2006) 922–930.
[42] W. Chen, B.J. Qu, Chem. Mater. 15 (2003) 3208–3213.
[43] W. Chen, L. Feng, B.J. Qu, Chem. Mater. 16 (2004) 368–370.
[44] W. Chen, L. Feng, B.J. Qu, Solid State Commun. 130 (2004) 259–263.
[45] M. Zanetti, G. Camino, R. Thomann, Polymer 42 (2001) 4501–4507.
[46] M. Zanetti, T. Kashiwangi, L. Falqui, G. Camino, Chem. Mater. 14 (2002) 881–887.
[47] J. Zhu, F.M. Uhl, A.B. Morgan, C.A. Wilkie, Chem. Mater. 13 (2001) 4649–4654.
[48] F.Z. Zhang, X. Xiang, F. Li, X. Duan, Catal. Surv. Asia 12 (2008) 253–265.
[49] K. Yamaguchi, K. Ebitani, K. Kaneda, J. Org. Chem. 64 (1999) 2966–2968.
[50] K. Yamaguchi, T. Mizugaki, K. Ebitani, K. Kaneda, New J. Chem. 23 (1999) 799–801.
[51] K. Motokura, N. Fujita, K. Mori, T. Mizugaki, K. Ebitani, K. Kaneda, J. Am. Chem. Soc. 127 (2005) 9674–9675.
[52] Y.Y. Ding, Z. Gui, J.X. Zhu, Y. Hu, Z.Z. Wang, Mater. Res. Bull. 43 (2008) 3212–3220.
[53] L.C. Du, B.J. Qu, J. Mater. Chem. 16 (2006) 1549–1554.
[54] O. Persenaire, M. Alexandre, P. Degée, P. Dubois, Biomacromolecules 2 (2001) 288–294.
[55] I. Noda, Appl. Spectrosc. 47 (1993) 1329–1336.
[56] I. Noda, J. Mol. Struct. 799 (2006) 2–15.
[57] I. Noda, J. Mol. Struct. 883 (2008) 2–26.
[58] B.J. Sun, Y.N. Lin, P.Y. Wu, H.W. Siesler, Macromolecules 41 (2008) 1512–1520.
[59] B.J. Sun, Q. Jin, L.S. Tan, P.Y. Wu, F. Yan, J. Phys. Chem. B 112 (2008) 14251–14259.